# MINI-RF BISTATIC DATA OBSERVATIONS FOR THE LUNAR SURFACE WATER-ICE DETECTION IN CABEUS CRATER REGION.

N. Verma[1], P. Mishra[2], N. Purohit[3]. [1]Physical Research Laboratory Ahmedabad, India (nidhiverma.iiita@gmail.com), [2,3] Indian Institute of Information Technology Allahabad, India.

**Introduction:** The Arecibo Observatory (AO) Planetary Radar transmitter and the Miniature Radio Frequency (MiniRF) radar onboard NASA's Lunar Reconnaissance Orbiter (LRO) were used as a receiver to collect bistatic data of the lunar surface [1, 2]. The bistatic data acquires bistatic radar measurements of the lunar surface to understand the radar scattering properties of different materials as a function of bistatic angle ($\beta$) [3]. Research based on a $\beta$ explains that this parameter is very sensitive to water-ice regions along with circular polarization ratio (CPR) greater than unity region, where CPR is the ratio of the same sense circular (SC) polarization to opposite sense circular (OC) polarization. Several radar-based investigations, including CPR, have identified the existence of water from polar regions of Mercury [4, 5], Jupiter, Mars [6], and Moon [7]. The higher value of CPR (CPR >1) can also be due to other reasons such as differentiation in density, particles, and voids in weakly absorbing media, e.g., water-ice [8, 9]. Further, studies revealed that CPR >1 was also occurred in rough surface regions due to the double bounce effect [9], [10, 11].

The preliminary research related to bistatic angle ($\beta$) and circular polarization ratio (CPR) indicates that these two parameters can be used simultaneously for determining water-ice on polar crater [12]. CPR from lunar surface scattering explains that high CPR due to a rocky surface will be relatively insensitive to the $\beta$, while high CPR due to water-ice will be very sensitive to $\beta$, with elevated CPR values dropping off abruptly at the bistatic angle greater than about 1°-2° [8]. Hence, the $\beta$ needs to be explored in more detail to find the possibilities of water–ice on the lunar polar crater. For this purpose, the region of interest has been classified into two classes rough and smooth regions using the fractal dimension approach [13]. Further, it has been observed that the $m$-$\delta$ decomposition method is also used in finding volume scattering parameters, which uses a degree of polarization ($m$) [14] and relative phase ($\delta$) concept. Low values of $m$ and $\delta$ values other than close to -90° (for surface scattering) and close to +90° (for dihedral scattering) represent volume scattering (associated with water-ice particles) [15]. Following this, CPR, $\beta$ and $m$-$\delta$ decomposition method have been applied to the rough and smooth regions. The findings of this research work eliminate the fact that the $\beta$ is less sensitive in the rough region, where CPR >1. Therefore, to accurately determine the behaviour of $\beta$, analysis was done in the smooth and rough region both.

**Data Description:** Bistatic Mini-RF is S-band (2.38 GHz) hybrid polarimetric Synthetic Aperture Radar (SAR) data. It provides raw data consisting of four channels such as $|E_{LH}|^2$ (transmit left circular polarized and received horizontally polarized signal), $|E_{LV}|^2$ (transmit left circular polarized and received vertically polarized signal), the real part of ($E_{LH}E_{LV^*}$), the imaginary part of ($E_{LH}E_{LV^*}$), here * represents a complex conjugate. These raw data are available on the Geosciences Node of NASA's Planetary Data System (PDS). Along with raw data, the derived data is also available on PDS, which includes six bands, namely, latitude, longitude, bistatic angle ($\beta$), incidence angle, emission angle and Stokes parameters. The $\beta$ and Stokes parameters will be further used for the analysis of the lunar surface along with other parameters. The present work has been done on the Cabeus 1 crater region, which is located at the centre longitude and latitude 31.729°W, 78.817°S. The total backscatter power ($S_1$) image of the Cabeus-1 crater is shown in Fig. 1.

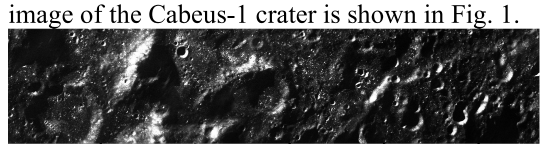

Fig. 1: Total backscatter power ($S_1$) image of Cabeus 1 crater region.

**Methodology and Results:**
This work aims to examine the criterion of bistatic angle ($\beta$) and circular polarization ratio (CPR) for detection of water-ice deposits in the Cabeus 1 crater region. To this end, first, we will classify the lunar surface into two regions, namely rough and smooth, based on the fractal approach. Then CPR, $\beta$ values, and the volume scattering characteristics of these classified regions will be studied. In particular, the results and discussions on CPR >1 along with lower $\beta$ value criteria, volume scattering along with lower $\beta$ value criteria, and combined CPR >1, volume scattering along with lower $\beta$ value criteria will be presented.

*Classification of the lunar surface using the fractal approach*

The fractal dimension is obtained from the first Stoke parameter ($S_1$) [13]. The fractal dimension gives information about roughness properties. The mean value of fractal dimension has been found as 2.34 (window size 9×9) for the whole $S_1$ parameter image. Hence above the means values, pixels are considered as rough and below the mean value, pixels are considered as the smooth region. To classify fractal images into two classes, the k-means classifier was applied (1000 iterations). The two classes are respectively defined by a mean fractal dimension of 1.9 (smooth) and 2.47 (rough).

*Circular polarization ratio analysis (CPR)*

The existing literature considers the presence of water-ice deposits on the moon craters wherever CPR >1 [10]. The water-ice and rough surface region cannot be distinguished on the basis of CPR alone. For the considered crater region, it is observed that the above classified rough area and the smooth area has CPR >1 regions, as shown in Fig 2 (pixels in red color). Further, statistical analysis for $\beta$ was performed in CPR >1 for rough and smooth regions. From which, it can be concluded that the mean $\beta$ value is approximately similar in both regions (mean ± std value lies in between 2° to 4°). Based on the results, both rough and smooth lunar surfaces can contain possible water-ice.

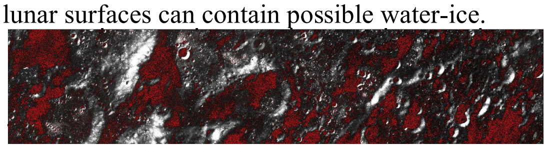

Fig. 2: Pixels (red) satisfying CPR >1 criteria are overlaid on the $S_1$ image of the south polar Cabeus 1 crater.

*Analysis of $m - \delta$ decomposition method*

The $m$-$\delta$ decomposition method is used to identify surface, double bounce, and volume scattering [16]. It has been observed that due to the dielectric mixing (i.e., water-ice particle), the dominant volume scattering occurs, and surface roughness gives double-bounce scattering behaviour. This scattering behaviour can be extracted using the $m$-$\delta$ decomposition method. The calculation of these scattering components can be done with the following equations

$$f_{surface} = \sqrt{0.5m(1 - \sin\delta)} \quad (1)$$

$$f_{double} = \sqrt{0.5m(1 - \sin\delta)} \quad (2)$$

$$f_{volume} = \sqrt{0.5S_1(1 - m)} \quad (3)$$

$$f_{volume} > f_{double} + f_{surface} \quad (4)$$

where $m$ is the degree of polarization and $\delta$ is the relative phase difference.

Equation 4 is satisfied for $m$ <0.32 for dominant volume scattering (possible water-ice region). Further, two regions have been obtained by taking the criterion $m$<0.32 for dominant volume scattering. Further, an analysis of $m$<0.32 was performed for rough and smooth regions as obtained after the fractal method. After obtaining the dominant volume scattering ($m$ <0.32) region, the analysis of $\beta$ has been performed. From the analysis of the bistatic angle ($\beta$), it has been observed that the value of $\beta$ is similar for rough and smooth regions.

*CPR >1 and m <0.32 combined analysis*

Further, from the analysis of the bistatic angle ($\beta$), results have been found using criteria CPR >1 and $m$ <0.32, as shown in Fig 3. These results show that the mean value of $\beta$ is less than 3° in both regions. Thus, it can be concluded that $\beta$ shows similar behaviour for rough and smooth regions.

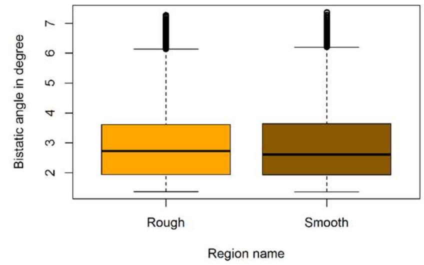


Fig. 3: Bistatic angle analysis in CPR >1 and $m$ <0.32.

**Conclusions**

The study of bistatic angle along with CPR, $m$–$\delta$ decomposition method, and then with the combined CPR and $m$-$\delta$ are undertaken. An interesting observation has been made that the bistatic angle possesses a similar behaviour in CPR greater than unity and degree of polarization less than 0.32 for rough and smooth regions. Analyzing the results presented here ultimately leads to the following important observations: 1) Both smooth and rough regions are likely to have the possibility of water-ice deposits, 2) to verify that water-ice deposits are indeed present on the lunar surface, further analysis is needed along with the physical, electrical and chemical properties of the moon's surface. In the future, Chandrayaan-2 SAR data from DFSAR [17] will be combined with Mini-RF bistatic observations for confirming the possibility of water-ice deposits.

**Acknowledgments:** The authors are thankful to Planetary Data System (PDS) for providing free Bistatic Mini-RF data for the Cabeus 1 crater region.

**References:**

[1] G. Patterson. et al. (2017) *Icarus*, *283*, 2-19. [2] B. Bussey. et al. (2012) *AGU Fall Meeting Abstracts*, P43B-1919. [3] D. E. Wahl. et al. (2012), Algorithms for Synthetic Aperture Radar Imagery XIX, 83940D. [4] B. J. Butler. et al.(1993), JGR Planets, *98*, 15003-15023. [5] M. A. Slade et. al. (1992) *Science*, *258*, 635-640. [6] L. Carter. et al. (2012), 4285. [7] N. Verma. et al. (2018) *IEEE IGARSS*, 4567-4570. [8] P. Spudis. et al. (2010) *Geophysical Research Letters*, 37. [9] C. Neish. et al. (2011), *JGR Planets*, *116*, 2011. [10] Y.-Q. Jin and N. Liu (2017), *IEEE IGARSS*, 4926-4927. [11] W. Fa and V. R. Eke (2018) *JGRS Planets*, *123*, 2119-2137. [12] C. L. Lichtenberg (2000), The Johns Hopkins University. [13] P. Mishra et al. (2014), *IEEE JSTAR*, *8*, 30-38. [14] V. Kumar. et al. (2017) *IEEE IGARSS*, 1028-1031. [15] R. Shirvany. et al. (2012) *IEEE TGRS*, *51*, 539-551. [16] R. K. Raney (2007) *IEEE TGRS*, *45*, 3397-3404. [17] S. Bhiravarasu, et al. (2021) *LPSC*, 1787.